SUPPLEMENTAL MATERIAL

Huang et al., https://doi.org/10.1084/jem.20171413

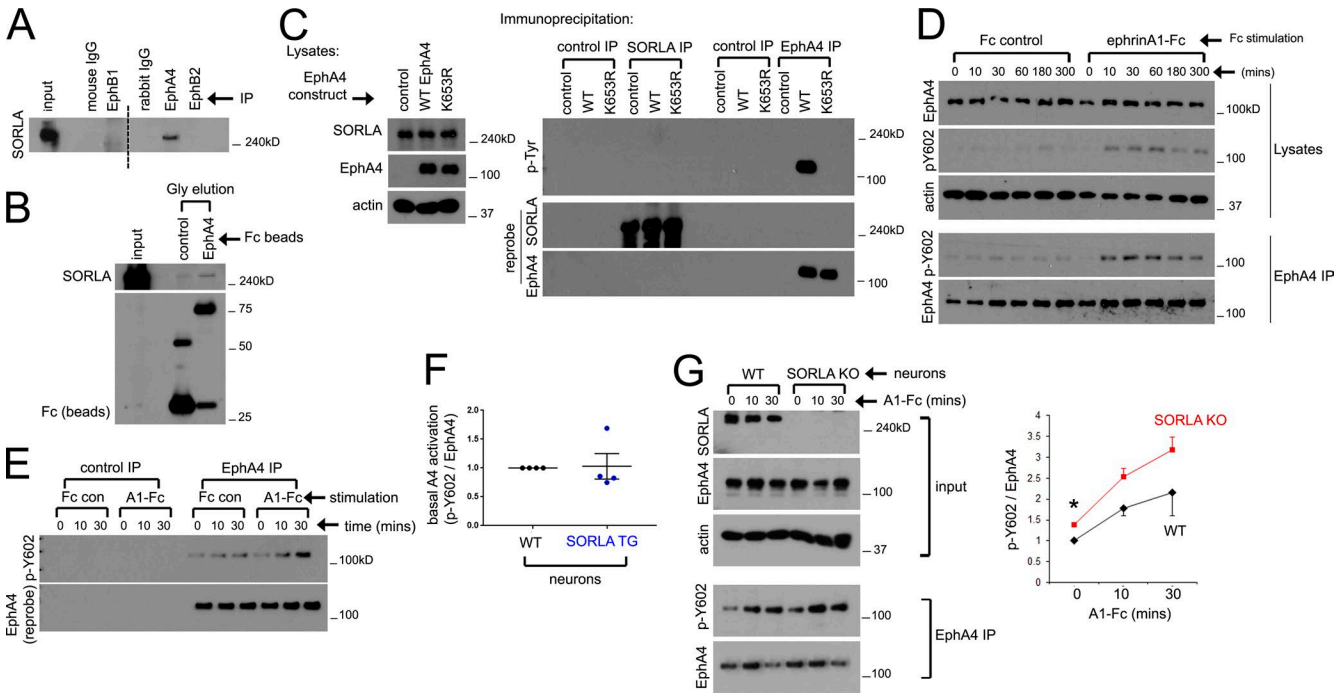

Figure S1. **SORLA affects EphA4 activation.** (A) Screening of Eph receptor immunoprecipitates for SORLA interaction. WT mouse brain lysates were coimmunoprecipitated with control antibodies or EphB1, EphA4, or EphB2, and immunoprecipitates were immunoblotted for SORLA. Dashed line indicates non-adjacent lanes in the blot. (B) SORLA interacts with the EphA4 ectodomain. Control or EphA4-Fc immobilized on protein G Sepharose was incubated with cell lysates overexpressing SORLA, and coprecipitation of SORLA was detected by immunoblot. (C) SORLA is not an EphA4 substrate. Vector control, WT, or a K563R kinase dead EphA4 mutant constructs were transfected into HEK293T cells. Lysates were immunoblotted for EphA4 (left) or immunoprecipitated with control, SORLA, or EphA4 antibodies, and immunoprecipitates were immunoblotted for phosphotyrosine (right). Blots from the immunoprecipitates were then reprobed with SORLA or EphA4 antibodies (bottom). (D and E) EphrinA1 stimulation results in prolonged EphA4 activation. HEK293 cells stably expressing EphA4 (D) or primary cortical neurons (E) were incubated with ephrinA1-Fc or Fc control for the time indicated, EphA4 was immunoprecipitated from lysates, and the immunoprecipitates were probed for pY602 or EphA4. (F) Steady-state EphA4 activation levels are comparable between control and SORLA TG neurons. pY602/EphA4 ratios in EphA4 immunoprecipitates from WT and SORLA TG (TG) cortical neurons were measured without ephrinA1-Fc stimulation (mean ± SE from four independent experiments). (G) EphA4 activation is enhanced in SORLA KO neurons. WT and SORLA KO neurons were stimulated with ephrinA1-Fc (A1-Fc) for the time indicated, and EphA4 was immunoprecipitated from neuronal lysates and immunoblotted for pY602 or EphA4. Graph represents mean ± SE from three independent experiments ($n = 3$; *, $P < 0.005$; Student's t test).

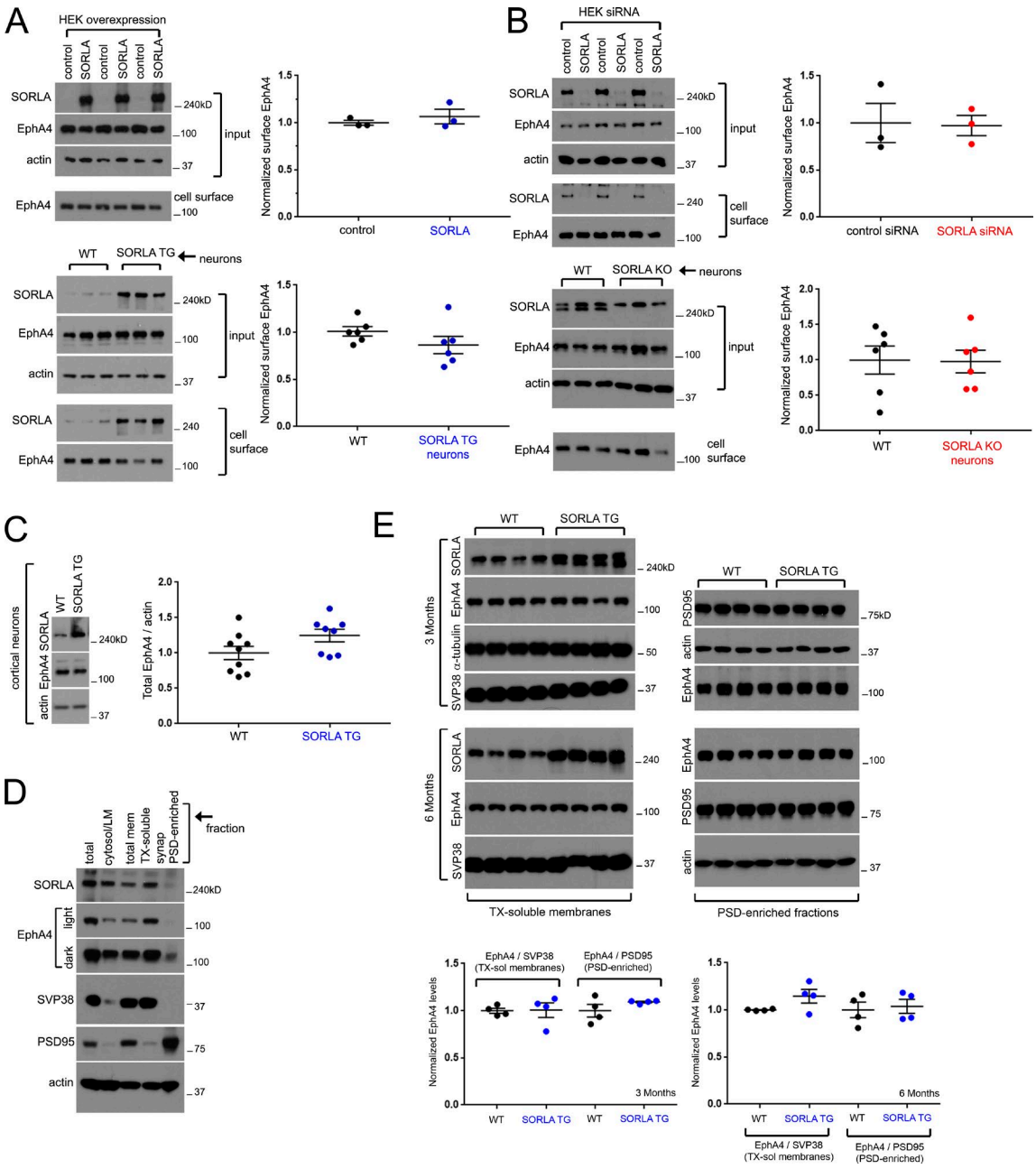

Figure S2. **Steady-state EphA4 cell surface levels are not affected by SORLA, and total/membrane-associated EphA4 levels are similar with SORLA overexpression in neurons and SORLA TG mice.** (A) SORLA overexpression does not affect the levels of EphA4 on the cell surface. HEK293T cells transfected with control/SORLA overexpression vectors (top) or WT/SORLA TG cortical neurons (bottom) were subjected to cell-surface biotinylation, and labeled proteins were precipitated with streptavidin agarose and immunoblotted for EphA4. (B) SORLA depletion or KO does not affect surface EphA4 levels. HEK293T cells transfected with control or SORLA siRNA oligonucleotides (top) or WT/SORLA KO cortical neurons (bottom) were subjected to cell-surface biotinylation as in A, and surface EphA4 levels were examined by immunoblotting. In A and B, top graphs represent (from HEK experiments) mean ± SE from three replicates, and bottom graphs (from cortical neurons) represent six replicates from two independent experiments. (C) Total EphA4 levels are unaffected in SORLA TG neurons. EphA4 levels were determined in cultured WT and SORLA TG cortical neurons by immunoblotting, and EphA4/actin ratios normalized to WT neurons were plotted (mean ± SE; plots are from nine individual replicate cultures in three independent experiments). (D) Hippocampal tissue from a WT mouse was subjected to biochemical membrane separation to separate synaptosomes and presynaptic and postsynaptic enriched protein components. Equal protein quantities were loaded and immunoblotted for the components indicated. (E) Hippocampal tissue from WT and SORLA TG mice were collected at 3 and 6 mo and subjected to fractionation for Triton X-100–soluble (TX-soluble) membranes and PSD-enriched fractions. Relative EphA4 values normalized to synaptophysin (SVP38) and PSD95 were plotted normalized to WT values (set to 1.0; mean ± SE from four age-/litter-matched animals of each age/genotype/fraction).

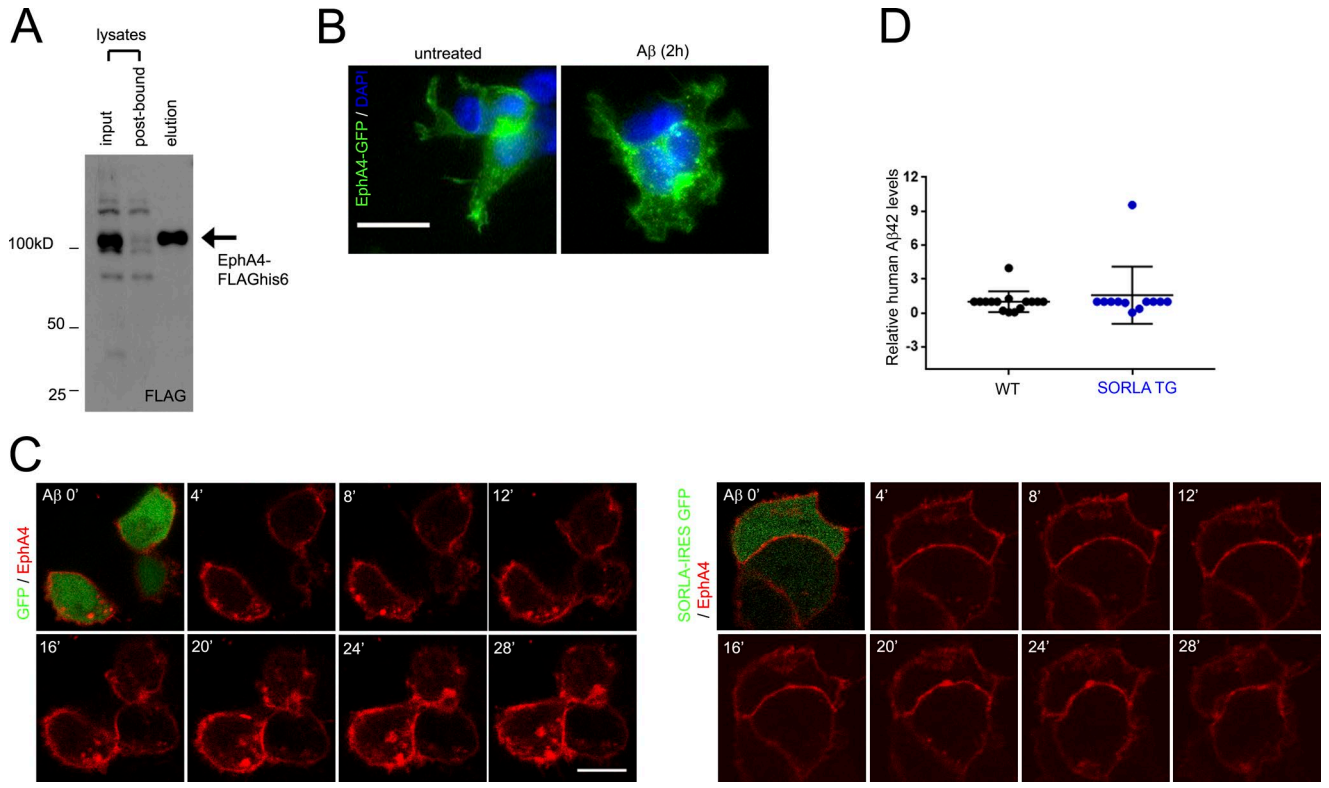

Figure S3. **EphA4 purification and clustering.** (A) A vector expressing EphA4-FLAGhis6 was transfected into HEK293T cells, and cell lysates were incubated with Ni-NTA agarose. Equal volumes of the lysate input before and after (post-bound) Ni-NTA binding and eluates in 0.3 M imidazole were immunoblotted for FLAG. (B) HEK293T cells were transfected with constructs expressing EphA4-GFP (green) and incubated with 500 nM Aβ for 2 h. Bar, 10 µm. (C) SORLA attenuates Aβ-dependent EphA4 clustering. HEK293T cells were cotransfected with vectors expressing EphA4-mCherry (red) and GFP (left) or SORLA-IRES-GFP (right) and exposed to 500 nM Aβ. Images were acquired by confocal live-cell imaging immediately at time 0 and continuously captured at the time points indicated. Bar, 10 µm. (D) SORLA overexpression has no effect on Aβ clearance or catabolism in vivo. Hippocampal tissue from $Aβ_{1–42}$-injected WT and SORLA TG mice subjected to Morris water maze analysis were subjected to $Aβ_{1–42}$ extraction and analysis using an ELISA system for human $Aβ_{1–42}$. Relative $Aβ_{1–42}$ levels were normalized to WT $Aβ_{1–42}$ (set to 1.0; n = 15 WT and n = 12 SORLA TG animals); graph represents mean ± SD.

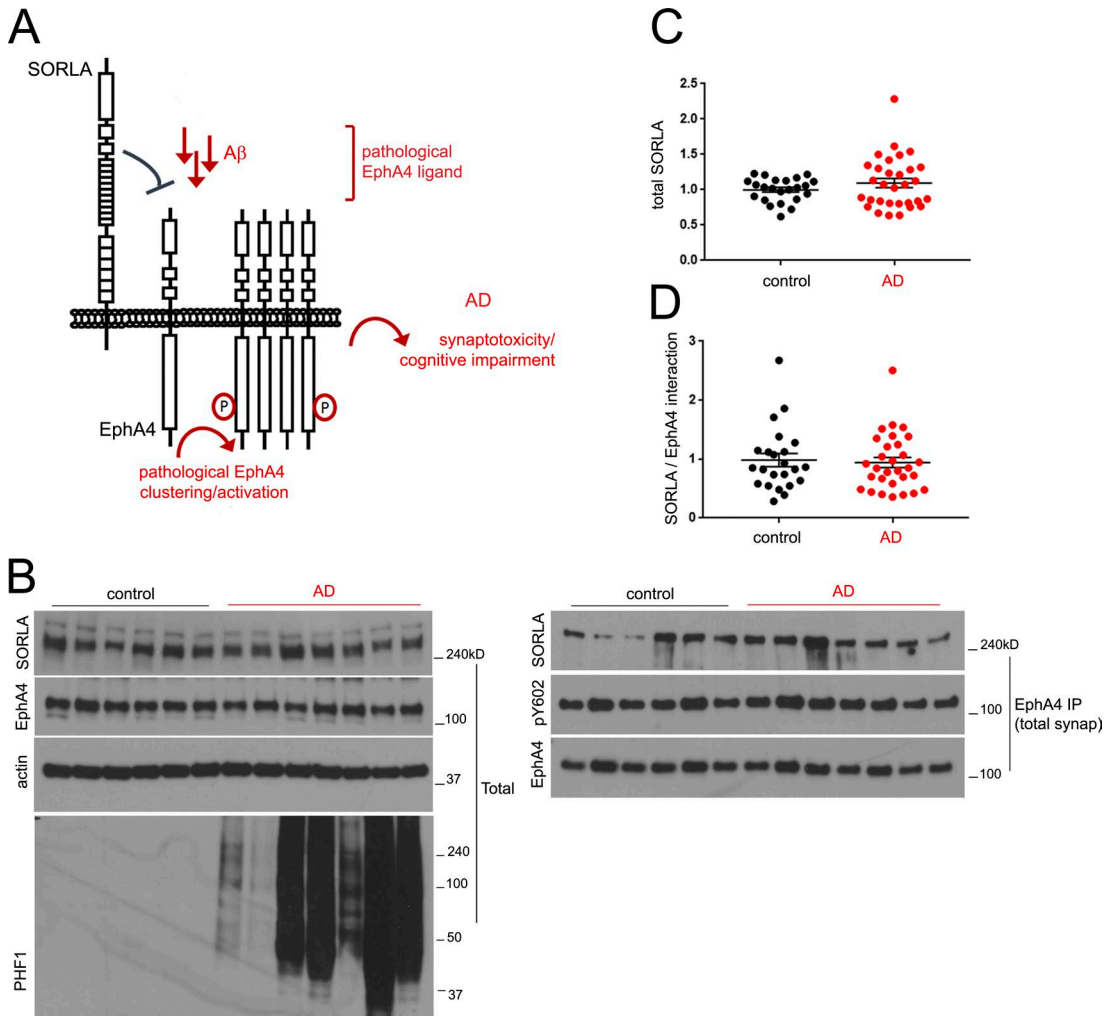

Figure S4. **Variability in total SORLA levels and association with EphA4 in control and AD populations.** (A) A model for SORLA-mediated attenuation of EphA4 activation in response to Aβ. SORLA and EphA4 interact, which attenuates EphA4 clustering and activation in response to Aβ (red), which attenuates downstream synaptotoxic effects in AD. (B–D) Testing the model for SORLA/EphA4 interaction in human AD. (B) Immunoblot of total brain tissue lysates and EphA4 immunoprecipitates from total synaptosomes isolated from representative control and AD patient cohorts. (C) SORLA levels from total brain lysates in control and AD brain. (D) SORLA/EphA4 ratios in EphA4 immunoprecipitates derived from control and AD brain. Graphs in C and D indicate individual data points; mean ± SE (control, $n = 23$; AD, $n = 30$).

Table S1. **List of human brain tissues used**

Number	Source	Identifier	Diagnosis	Sex	Age	Braak stage
					yr	
1	UCSD	X5709	Normal	M	94	2
2	UCSD	X5628	Normal	F	80	1
3	UCSD	X5248	Normal	F	93	1
4	UCSD	X5114	Normal	M	87	1.1
5	UCSD	X5070	Normal	F	97	1
6	UCSD	X5049	Normal	F	102	1
7	UCSD	X4996	Normal	M	91	3
8	UCSD	X4954	Normal	M	76	0
9	UCSD	X5732	AD	F	78	6.2
10	UCSD	X5725	AD	F	66	6.2
11	UCSD	X5720	AD	F	77	6.2
12	UCSD	X5707	AD	M	82	6.2
13	UCSD	X5704	AD	M	77	6.2
14	UCSD	X5698	AD	F	77	6.2
15	UCSD	X5693	AD	F	78	6.2
16	UCSD	X5691	AD	F	62	6.2
17	UCSD	X5689	AD	F	74	6.2
18	UCSD	X5686	AD	M	88	6.2
19	UCSD	X5685	AD	F	88	6.2
20	UCSD	X5684	AD	M	68	6.2
21	UCSD	X5680	AD	M	84	6.2
22	UCSD	X5302	Normal	F	83	1.1
23	UCSD	X5130	Normal	M	71	1
24	UCSD	X5006	Normal	M	69	0
25	UCSD	X4942	Normal	M	83	0
26	UCSD	X4689	Normal	F	79	0
27	UCSD	X5754	AD	M	92	6.2
28	UCSD	X5743	AD	M	87	6.2
29	UCSD	X5738	AD	F	85	6.2
30	UCSD	X5667	AD	F	71	6.2
31	UCSD	X5658	AD	F	70	6.2
32[a]	UMiami	HCTZZA_16_009	Normal	M	89	
33	UMiami	HCTZZC_16_009	Normal	F	82	
34	UMiami	HCTZZH_16_010	Normal	F	65	
35	UMiami	HCTZZV_16_001	Normal	F	86	
36	UMiami	HBDE16_16_03	Normal	M	83	
37	UMiami	HCTZZR_16_006	AD	M	86	III–IV
38	UMiami	HBCG_16_003	AD	F	90	III–IV
39	UMiami	HBED_16_004	AD	F	71	III–IV
40	UMiami	HBEK_16_001	AD	F	77	V–VI
41	UMiami	HBFF_16_004	AD	M	85	III–IV
42	UMiami	HBFP_16_001	AD	F	83	V–VI
43	UMiami	HBFR_16_001	AD	F	69	V–VI
44	UMiami	HCTYH_16_013	Normal	F	71	
45	UMiami	HCTYP_16_019	Normal	M	75	
46	UMiami	HCTYY_16_006	Normal	M	90	
47	UMiami	HCTZL_16_005	Normal	F	65	
48	UMiami	HCT15HAB16_016	Normal	M	67	
49	UMiami	HCTZT_16_006	Normal	M	76	
50	UMiami	HCTYN_16_001	AD	F	80	V–VI
51	UMiami	HCTZX_16_001	AD	M	95	V–VI
52	UMiami	HCTZZF_16_004	AD	F	103	III–IV
53	UMiami	HBBX_16_001	AD	F	94	V–VI
54	UMiami	HBDA_16_001	AD	M	80	V–VI
55	UMiami	HBDM_16_001	AD	M	60	V–VI
56	UMiami	HBEC_16_001	AD	M	71	V–VI

UCSD, University of California, San Diego; UMiami, University of Miami.
[a]32–43 are samples (in order, left to right) in Fig. 7; 44–56 are samples in Fig. S4.